

Tests of reinforced concrete deep beams

Wen-Yao Lu^{*1}, Hsin-Tai Hsiao^{2b}, Chun-Liang Chen^{1c}, Shu-Min Huang^{1c}
and Ming-Che Lin^{1c}

¹Department of Interior Design, China University of Technology, Taipei 11695, Taiwan, R.O.C.

²Department of Civil Engineering, China University of Technology, Taipei 11695, Taiwan, R.O.C.

(Received January 17, 2013, Revised February 11, 2014, Accepted February 18, 2014)

Abstract. This study reports the test results of twelve reinforced concrete deep beams. The deep beams were tested with loads applied through and supported by columns. The main variables studied were the shear span-to-depth ratios, and the horizontal and vertical stirrups. The shear strengths can be effectively enhanced for deep beams reinforced with both horizontal and vertical stirrups. The test results indicate the shear strengths of deep beams increase with the decrease of the shear span-to-depth ratios. The normalized shear strengths of the deep beams did not increase proportionally with an increase in effective depth. An analytical method for predicting the shear strengths of deep beams is proposed in this study. The shear strengths predicted by the proposed method and the strut-and-tie model of the ACI Code are compared with available test results. The comparison shows the proposed method can predict the shear strengths of reinforced concrete deep beams more accurately than the strut-and-tie model of the ACI Code.

Keywords: deep beams; shear strength; strut-and-tie

1. Introduction

In the real structure, the deep beams had loads applied through and supported by columns. However, most experimental work on deep beams had been with loads applied through and supported by bearing plates (Yang 2010; Mihaylov *et al.* 2010; Tuchscherer *et al.* 2010; Tuchscherer *et al.* 2011). Due to the significant rigidity of the load-column, the critical sections for flexure of the deep beams were at the faces of the load-column (Lu *et al.* 2012).

Only three studies were found discussing deep beams tested with loads applied through and supported by columns (Rogowsky *et al.* 1986; Foster and Gilbert, 1998; Lu *et al.* 2012). Further experimental work on deep beams tested with loads applied through and supported by columns should be performed.

The strut-and-tie model of the ACI Code (2011) is the main design document for deep beams. The shear strength of deep beams tested with loads applied through and supported by bearing plates was accurately predicted by Russo *et al.* (2005) and Lu *et al.* (2010). The behavior of the

*Corresponding author, Professor, E-mail: luwenyao@cute.edu.tw

^aProfessor

^bAssociate Professor

^cInstructor

prestressed concrete deep beams tested with loads applied through and supported by bearing plates can be well simulated by Kim *et al.* (2012). However, the analytical method in predicting the shear strength of deep beams with loads applied through and supported by columns is still very limited. In this study, twelve tested deep beams will be first presented, and then the analytical method for predicting the shear strengths of deep beams will be proposed.

2. Experimental study

In this study, 12 reinforced concrete deep beams tested with loads applied through and supported by columns.

2.1 Specimen details

Typical deep beam specimens are shown in Fig. 1. The length (L), width (b), overall depth (h) and effective depth (d) of the tested deep beams were 700 mm, 100 mm, 300 mm and 270 mm, respectively. The shear span-to-depth ratio (a/d), compressive strength of concrete (f'_c), flexural steel, horizontal and vertical stirrups are listed in Table 1. The flexural steel consisting of 2-#5 straight bars were welded to anchored plates at the ends of the beam to prevent local bond failures (Fig. 1). The dimensions of the anchored plates were 100 mm by 60 mm by 6 mm. To prevent bearing failures, the top of the load-columns was welded to a 150 mm by 100 mm by 6 mm steel plate, and the bottoms of the support-columns were welded to a 150 mm by 50 mm by 6 mm steel plate (Fig. 1).

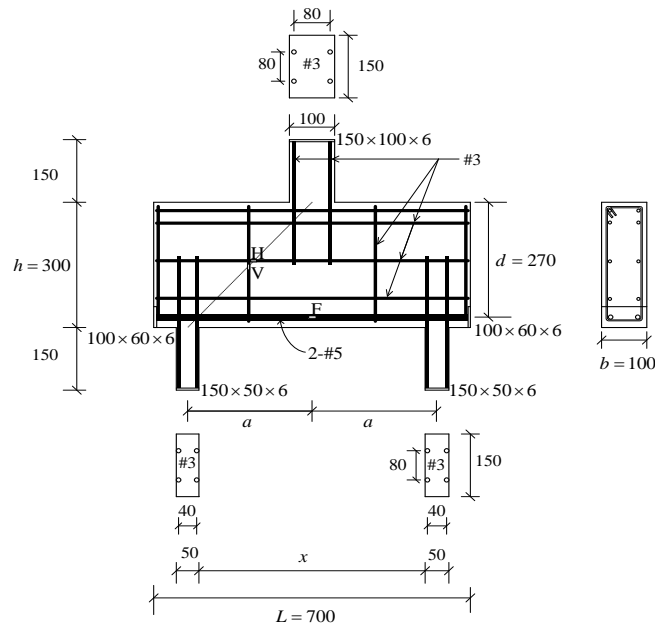


Fig. 1 Details of typical specimens (Unit: mm)

Tests of reinforced concrete deep beams

Table 1 Specimen details

Beam No.	L (mm)	a (mm)	b (mm)	d (mm)	a/d	f'_c (MPa)	Flexural steel	Horizontal stirrups	Vertical stirrups
1	700	300	100	270	1.11	37.2	2-#5	-	-
2	700	200	100	270	0.74	37.2	2-#5	-	-
3	700	150	100	270	0.56	37.2	2-#5	-	-
4	700	300	100	270	1.11	37.2	2-#5	3-#3	-
5	700	250	100	270	0.93	37.2	2-#5	3-#3	-
6	700	300	100	270	1.11	37.2	2-#5	-	1-#3
7	700	250	100	270	0.93	37.2	2-#5	-	1-#3
8	700	200	100	270	0.74	37.2	2-#5	-	1-#3
9	700	150	100	270	0.56	37.2	2-#5	-	1-#3
10	700	300	100	270	1.11	37.2	2-#5	3-#3	1-#3
11	700	250	100	270	0.93	37.2	2-#5	3-#3	1-#3
12	700	200	100	270	0.74	37.2	2-#5	3-#3	1-#3

Table 2 Properties of reinforcement

No.	f_y (MPa)	Remark
#3	390 MPa	Horizontal and vertical stirrups, Main bars of columns
#5	374 MPa	

Table 3 Properties of concrete

Design strength	Mean strength	Water-cement ratio	Slump	Coarse aggregate	Unit weight
34.6 MPa	37.2 MPa	0.45	150 mm	13 mm	2411 kg/m ³

The yield strength (f_y) of #3 reinforcement is 390 MPa, while the yield strength of #5 reinforcement is 374 MPa (Table 2). The properties of the concrete used in this study are shown in Table 3. The design strength of the concrete is 34.6 MPa, and the mean strength of the concrete is 37.2 MPa (Table 3).

2.2 Testing procedures

During the test, the strains in the flexural bars, horizontal and vertical stirrups of the deep beams were measured at locations F, H and V; respectively (Fig. 1), using electrical resistance gauges. Prior to testing, both surfaces of the deep beams were whitewashed to aid observation of crack development during the test. The setup for testing the deep beam is shown in Fig. 2. The beams were simply supported and tested in a 1000 kN capacity universal testing machine under static loading. The displacement was measured using a linear variable differential transformer



Fig. 2 Testing arrangements for deep beams

(LVDT) mounted on the bottom face at the mid-span of the beam, as seen in Fig. 2. For each load increment, the test data were captured by a data logger and automatically stored.

2.3 Test results

Based on the observation of photos of the deep beams tested with loads applied through and supported by columns at failure (Fig. 3), the applied load were transmitted along the path $E \rightarrow F \rightarrow G \rightarrow H$. Due to the significant rigidity of the load-column, the critical sections for flexure of the deep beams were at the faces of the load-column, as shown in Fig. 3. The shear action in the deep beams with loads applied through and supported by columns led to compression in a diagonal direction along \overline{FG} and tension perpendicular to the \overline{FG} direction (Fig. 3). The first inclined crack was formed in a diagonal direction along \overline{FG} at about 50 % of the ultimate load, and then the flexural cracks were formed near the mid-span of the deep beams. As the applied load increased, more diagonal cracks approximately parallel to the original ones developed with simultaneous widening and extension of the existing cracks. However, the deep beams did not fail immediately due to the occurrence of inclined cracks. After inclined cracking, the concrete between the inclined cracks can be represented as a concrete compression strut. The external shear was transferred by the concrete compression strut, and the possible failure mode will be a diagonal compression failure.

The observed load versus steel strains in a typical specimen (No. 12) is shown in Fig. 4. As can be seen in Fig. 4, the flexural steel and vertical stirrups did not yield at the ultimate state, while the horizontal stirrups yielded at the ultimate state. The observed load-displacement relationships for the 12 specimens are shown in Fig. 5. Apparently, the load-displacement curves were nearly linear up to the ultimate loads. It can be seen the deep beams tested in this study were not failed by flexure due to the non-ductile load-displacement relationships (Fig. 5). Since each flexural bar of the tested deep beams did not yield at the ultimate state, the failure mode of those beams can thus be recognized as diagonal compression failure (Table 4). The measured shear strength, $V_{bv, test}$, for each specimen obtained in the tests is summarized in Table 4. The test results show the smaller the shear span-to-depth ratio, the higher the shear strength of the deep beams is (Table 4). The shear strengths can be effectively enhanced for deep beams reinforced with both horizontal and vertical stirrups.

Tests of reinforced concrete deep beams

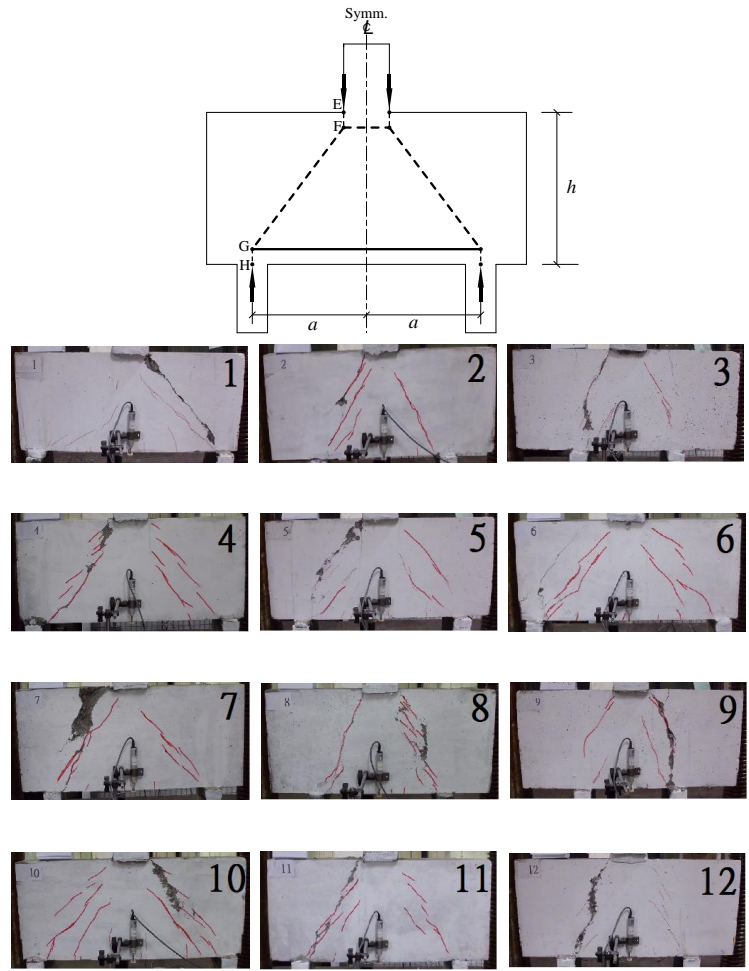


Fig. 3 Photos of deep beams at failure

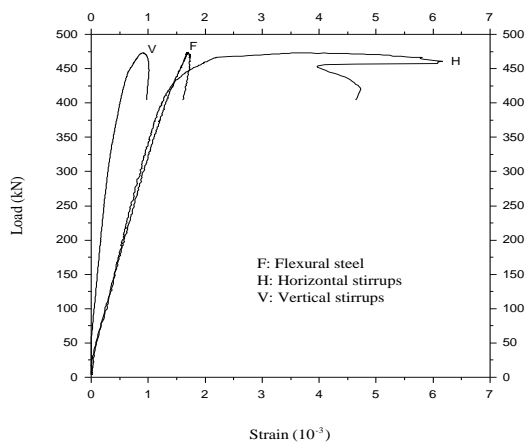


Fig. 4 Loads versus steel strain in typical specimen (No. 12)

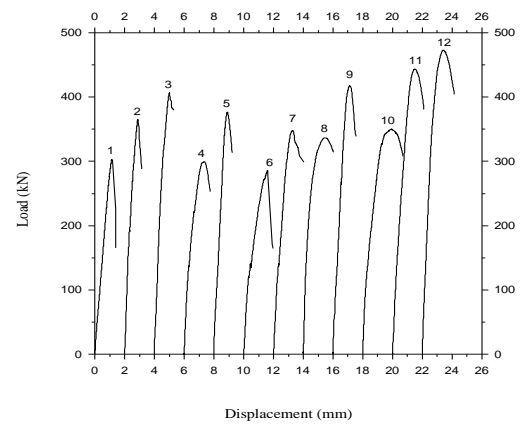


Fig. 5 Load versus displacement relationships

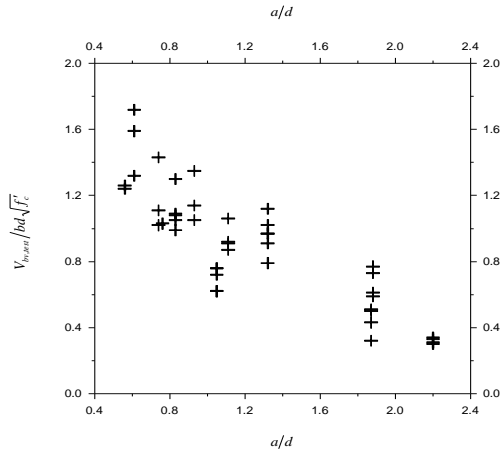


Fig. 6 Effect of shear span-to-depth ratios on the normalized shear strength of deep beams

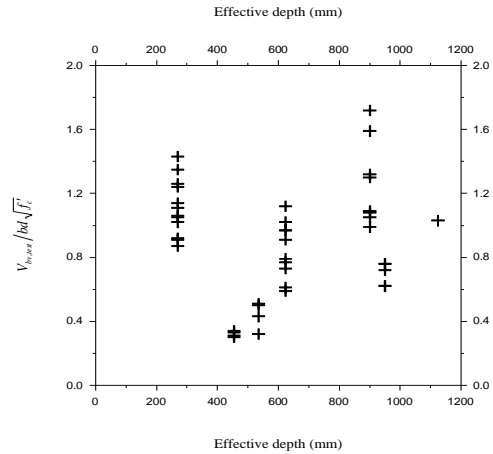


Fig. 7 Effect of the effective depth on the normalized shear strength of deep beams

Table 4 Test results

Beam No.	a (mm)	b (mm)	d (mm)	f'_c (MPa)	a/d	ρ_h^+ (%)	ρ_v^{++} (%)	$V_{bv, test}$ (kN)	$\frac{V_{bv, test}}{bd\sqrt{f'_c}}$	Failure mode ⁺⁺⁺
1	300	100	270	37.2	1.11	0	0	150.9	0.92	DC
2	200	100	270	37.2	0.74	0	0	182.3	1.11	DC
3	150	100	270	37.2	0.56	0	0	203.4	1.24	DC
4	300	100	270	37.2	1.11	1.58	0	149.5	0.91	DC
5	250	100	270	37.2	0.93	1.58	0	188.2	1.14	DC
6	300	100	270	37.2	1.11	0	0.48	142.6	0.87	DC
7	250	100	270	37.2	0.93	0	0.57	173.5	1.05	DC
8	200	100	270	37.2	0.74	0	0.71	168.1	1.02	DC
9	150	100	270	37.2	0.56	0	0.95	208.3	1.26	DC
10	300	100	270	37.2	1.11	1.58	0.48	174.9	1.06	DC
11	250	100	270	37.2	0.93	1.58	0.57	222.0	1.35	DC
12	200	100	270	37.2	0.74	1.58	0.71	236.2	1.43	DC

⁺ ρ_h : ratio of the horizontal stirrup, ⁺⁺ ρ_v : ratio of the vertical stirrups, ⁺⁺⁺ DC: Diagonal compression failure

The test results of previous studies (Rogowsky *et al.* 1986; Foster and Gilbert, 1998; Lu *et al.* 2012) are shown in Table 5. To examine the size effect on shear strength of deep beams, the normalized shear strength ($V_{bv, test} / \sqrt{f'_c} bd$) is defined as the measured shear strength divided by the square root of the compressive strength of concrete and the shear area. In comparison with the test results of this study and previous study, the size effect on the normalized shear strength is not obvious (Tables 4, 5). The shear span-to-depth ratio is the most important factor influencing the normalized shear strengths of the deep beams. The normalized shear strengths of 44 deep beams listed in Tables 4 and 5 are plotted

Tests of reinforced concrete deep beams

Table 5 Test results of previous study

Author	Beam No.	a/d	f'_c MPa	L (mm)	b (mm)	d (mm)	$V_{bv, test}$ (kN)	$\frac{V_{bv, test}}{bd\sqrt{f'_c}}$
Rogowsky <i>et al.</i> (1986)	BM1/1.0N	1.05	26.1	2200	200	950	602	0.62
	BM1/1.0S	1.05	26.1	2200	200	950	699	0.72
	BM2/1.0N	1.05	26.8	2200	200	950	750	0.76
	BM2/1.0S	1.05	26.8	2200	200	950	750	0.76
	BM1A/1.0S	1.05	26.1	2200	200	950	600	0.62
	BM1/1.5N	1.87	42.4	2200	200	535	354	0.51
	BM1/1.5S	1.87	42.4	2200	200	535	303	0.43
	BM2/1.5N	1.87	42.4	2200	200	535	348	0.50
	BM2/1.5S	1.87	42.4	2200	200	535	226	0.32
	BM1/2.0N	2.20	43.2	2200	200	455	199	0.33
	BM1/2.0S	2.20	43.2	2200	200	455	177	0.30
	BM2/2.0N	2.20	43.2	2200	200	455	204	0.34
	BM2/2.0S	2.20	43.2	2200	200	455	185	0.31
Foster and Gilbert (1998)	B1.2-3	0.76	80	1450	125	1124	1300	1.03
	B2.0-1	1.32	83	1400	125	624	795	1.12
	B2.0-2	1.32	120	1400	125	624	825	0.97
	B2.0-3	1.32	78	1400	125	624	700	1.02
	B2.0B-5	1.32	89	1400	125	624	585	0.79
	B2.0C-6	1.32	93	1400	125	624	730	0.97
	B2.0D-7	1.32	104	1400	125	624	720	0.91
	B3.0-1	1.88	80	2100	125	624	510	0.73
	B3.0-2	1.88	120	2100	125	624	525	0.61
	B3.0-3	1.88	77	2100	125	624	525	0.77
B3.0B-4	1.88	89	2100	125	624	435	0.59	
Lu <i>et al.</i> (2012)	C1	0.83	34.6	1700	200	900	1156	1.09
	C2	0.83	34.6	1700	200	900	1375	1.30
	C3	0.61	58.5	1300	170	900	1542	1.32
	C4	0.61	58.5	1300	170	900	1859	1.59
	C5	0.61	58.5	1300	170	900	2018	1.72
	C6	0.83	67.8	1700	200	900	1474	0.99
	C7	0.83	67.8	1700	200	900	1600	1.08
	C8	0.83	67.8	1700	200	900	1563	1.05

versus their shear span-to-depth ratio in Fig. 6. As can be seen in Fig. 6, the normalized shear strength of the deep beams decreased with the increase in the shear span-to-depth ratio. The normalized shear strengths of 44 deep beams are plotted versus their effective depth in Fig. 7. As can be seen in Fig. 7, the normalized shear strengths of deep beams did not increase proportionally with an increase in effective depth.

3. Proposed method

Fig. 8 shows the loads acting on the deep beams and the force transmission mechanisms of the proposed method. By considering the distances between force couples (Fig. 8), the relation between the vertical and horizontal shears can be expressed as follows:

$$\frac{V_{bv}}{V_{bh}} \approx \frac{jd}{a'} \quad (1)$$

where V_{bv} is the vertical shear force, V_{bh} is the horizontal shear force, jd is the length of the lever arm from the resultant compressive force to the centroid of the flexural steel, and a' is the actual shear span. According to the linear bending theory, the lever arm jd can be estimated as

$$jd = d - kd/3 \quad (2)$$

Considering a triangular stress block (Fig. 8), where kd is the depth of the compression zone at the section, and coefficient k can be defined as

$$k = \sqrt{[n\rho + (n-1)\rho']^2 + 2[n\rho + (n-1)\rho'd'/d]} - [n\rho + (n-1)\rho'] \quad (3)$$

where $n = E_s/E_c$ is the modular ratio of elasticity, E_s and E_c are the elasticity modulus of the steel and concrete, ρ is the ratio of the flexural bars, ρ' is the ratio of the compression reinforcement, and d' is the distance from the extreme compression fiber to the centroid of the compression reinforcement. The ratio of flexural steel and compression reinforcement can be defined as follows

$$\rho = \frac{A_s}{bd} \quad (4)$$

$$\rho' = \frac{A'_s}{bd} \quad (5)$$

where A_s and A'_s are the area of flexural steel and compression reinforcement of the deep beam.

As shown in Fig. 8, the critical sections for flexure were at the faces of the load-column, and the actual shear span a' can be calculated as

$$a' = a - \frac{a_c}{2} \quad (6)$$

where a_c is the width of the load-column.

Fig. 8 shows the proposed force transfer mechanism, which is composed of diagonal, horizontal and vertical mechanisms (Lu *et al.* 2010). The diagonal mechanism is a diagonal compression strut whose angle of inclination θ is defined as (Lu *et al.* 2010)

Tests of reinforced concrete deep beams

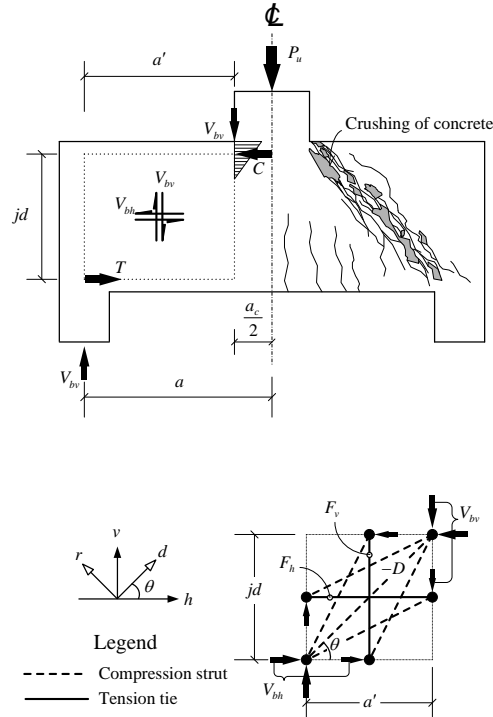


Fig. 8 Strut-and-tie for deep beams

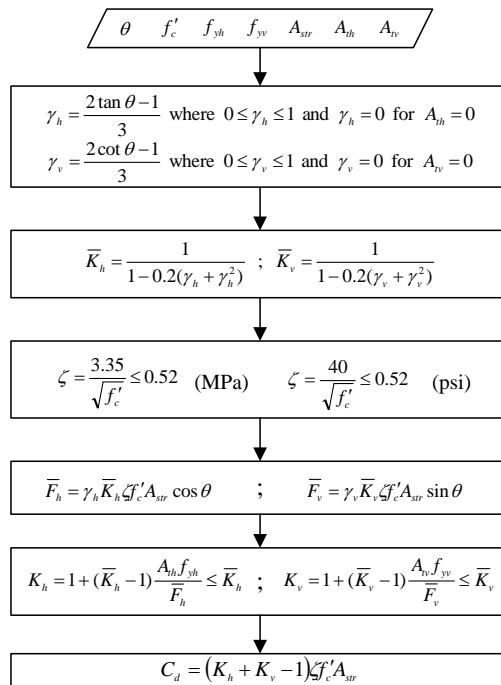


Fig. 9 Flow chart showing solution procedures

$$\theta = \tan^{-1}\left(\frac{jd}{d'}\right) \quad (7)$$

The effective area of the diagonal strut, A_{str} , can be estimated as

$$A_{str} = t_s \times b_s \quad (8)$$

where t_s is the thickness of the diagonal strut, and b_s is the width of the diagonal strut, which can also be taken as the width of the deep beam.

The thickness of the diagonal strut (t_s) depends on its end condition provided by the compression zone at the section and the bearing block (Lu *et al.* 2010). When the load is applied through a load-column (Fig. 8), t_s is only taken as kd in the absence of a bearing plate at the critical section for flexure.

According to Lu *et al.* (2010), the diagonal compression strength of deep beams can be estimated as follows:

$$C_d = (K_h + K_v - 1)\zeta f'_c A_{str} \quad (9)$$

where C_d is the predicted diagonal compression strength, K_h is the horizontal tie index, K_v is the vertical tie index, and ζ is the softening coefficient of concrete in compression.

The horizontal tie index can be estimated as follows (Lu *et al.* 2010):

$$K_h = 1 + (\bar{K}_h - 1) \frac{A_{th} f_{yh}}{\bar{F}_h} \leq \bar{K}_h \quad (10)$$

where \bar{K}_h is the horizontal tie index with sufficient horizontal stirrups, A_{th} is the area of the horizontal tie, f_{yh} is the yield stress of the horizontal stirrups, and \bar{F}_h is the balance amount of horizontal tie force.

The vertical tie index can be estimated as follows (Lu *et al.* 2010):

$$K_v = 1 + (\bar{K}_v - 1) \frac{A_{tv} f_{yv}}{\bar{F}_v} \leq \bar{K}_v \quad (11)$$

where \bar{K}_v is the vertical tie index with sufficient vertical stirrups, A_{tv} is the area of the vertical tie, f_{yv} is the yield stress of the vertical stirrups, and \bar{F}_v is the balance amount of vertical tie force.

The solution algorithm for C_d is summarized in Fig. 9. The shear strength of the deep beams according to the diagonal compression failure can be calculated as

$$V_{bv,calc} = C_d \sin \theta \quad (12)$$

where $V_{bv,calc}$ is the predicted shear strength.

In the proposed method, the predicted shear strength should be less than the shear force according to the flexural strength of the deep beams. The predicted shear strength of the deep beam according to the flexure failure can be determined as follows:

$$V_{bv,calc} = \frac{M_n}{a'} \quad (13)$$

where M_n is the nominal moment strength of the deep beam.

The nominal moment strength of the deep beam can be estimated as (ACI, 2011)

$$M_n = A_s f_y \left(d - \frac{A_s f_y}{1.7 f'_c b} \right) \quad (14)$$

where f_y is the yielding strength of the flexural bars of the deep beam.

4. Experimental verification

Forty-four specimens and their test results were employed to verify the proposed analytical methods. Of them, 12 were deep beams tested in this study while 32 were deep beams tested previously by Rogowsky *et al.* (1986), Foster and Gilbert (1998) and Lu *et al.* (2012).

The accuracy of the proposed method is evaluated in terms of a strength ratio, which is defined as the ratio of the measured strength to the calculated strength. The test-to-theory comparisons of deep beams are presented in Table 6 to examine the validity and accuracy of the proposed method,

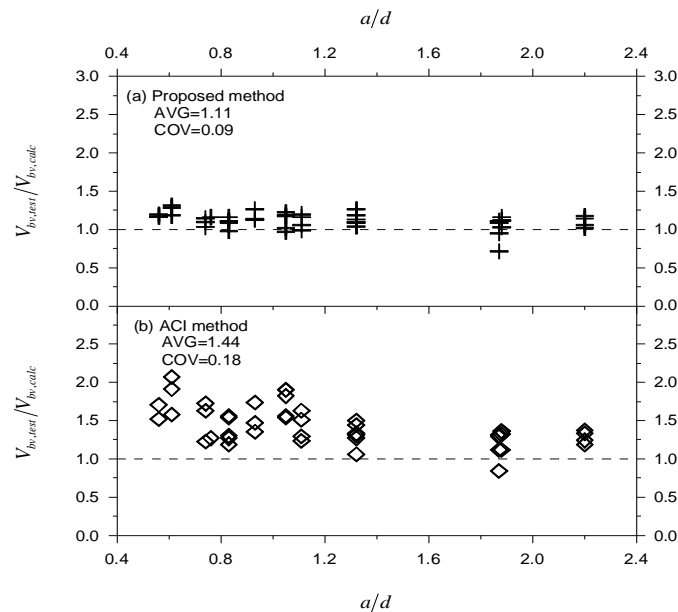


Fig. 10 Effect of shear span-to-depth ratios on shear strength predictions

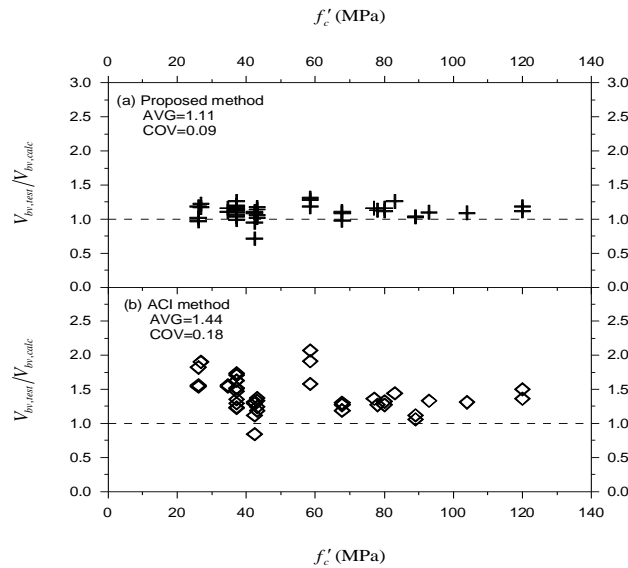


Fig. 11 Effect of compressive strengths of concrete on shear strength predictions

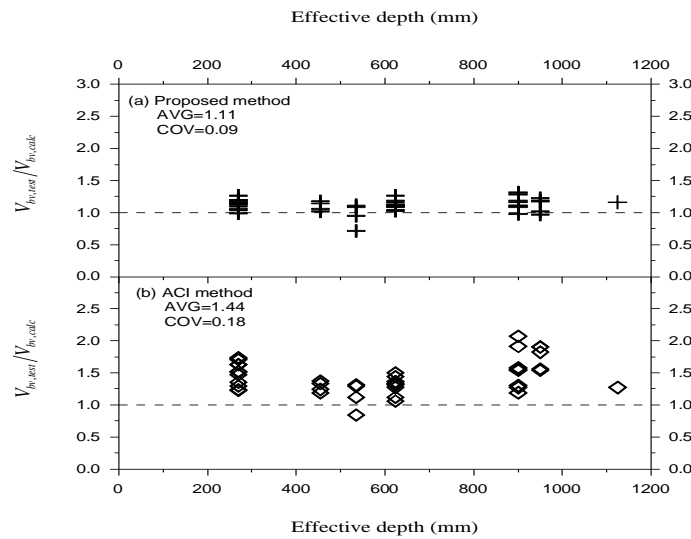


Fig. 12 Effect of effective depth on shear strength predictions

and the strut-and-tie model of the ACI Code (2011). Table 6 shows the mean of the measured-to-calculated strength ratios is 1.11 with a coefficient of variation of 0.09 for predictions using the proposed method, and the mean of the measured-to-calculated strength ratios is 1.44 with a coefficient of variation of 0.18 for predictions using the strut-and-tie model of the ACI Code (2011).

According to the experimental results of this study, the most important factor influencing the shear strength of deep beams is the shear span-to-depth ratio. The test-to-theory comparisons use parametric study to further assess the suitability of the proposed method, and the strut-and-tie

Tests of reinforced concrete deep beams

Table 6 Experimental verification

Beam No.	d mm	f'_c MPa	a/d	$\rho_h f_{yh}$ MPa	$\rho_v f_{yv}$ MPa	$V_{bv, test}$ kN	Proposed method		ACI method	
							$V_{bv, calc}$ kN	$\frac{V_{bv, test}}{V_{bv, calc}}$	$V_{bv, calc}$ kN	$\frac{V_{bv, test}}{V_{bv, calc}}$
This study										
1	270	37.2	1.11	-	-	150.9	130.0	1.16	92.5	1.63
2	270	37.2	0.74	-	-	182.3	159.6	1.14	112.0	1.63
3	270	37.2	0.56	-	-	203.4	174.0	1.17	119.4	1.70
4	270	37.2	1.11	6.16	-	149.5	141.0	1.06	115.7	1.29
5	270	37.2	0.93	6.16	-	188.2	166.7	1.13	128.0	1.47
6	270	37.2	1.11	-	1.87	142.6	144.6	0.99	115.7	1.23
7	270	37.2	0.93	-	2.22	173.5	153.0	1.13	128.0	1.36
8	270	37.2	0.74	-	2.77	168.1	162.7	1.03	137.2	1.23
9	270	37.2	0.56	-	3.71	208.3	174.0	1.20	137.2	1.52
10	270	37.2	1.11	6.16	1.87	174.9	146.0	1.20	115.7	1.51
11	270	37.2	0.93	6.16	2.22	222.0	175.2	1.27	128.0	1.73
12	270	37.2	0.74	6.16	2.77	236.2	215.5	1.10	137.2	1.72
Total							AVG	1.13		1.50
12							COV	0.07		0.13
Rogowsky et al. (1986)										
BM1/1.0N	950	26.1	1.05	-	0.86	602	618	0.97	385	1.56
BM1/1.0S	950	26.1	1.05	-	-	699	593	1.18	385	1.82
BM2/1.0N	950	26.8	1.05	0.34	0.86	750	641	1.17	395	1.90
BM2/1.0S	950	26.8	1.05	0.34	-	750	615	1.22	395	1.90
BM1A/1.0S	950	26.1	1.05	-	-	600	589	1.02	389	1.54
BM1/1.5N	535	42.4	1.87	-	1.09	354	319 +	1.11	270	1.31
BM1/1.5S	535	42.4	1.87	-	-	303	319 +	0.95	270	1.12
BM2/1.5N	535	42.4	1.87	4.35	1.09	348	319 +	1.09	270	1.29
BM2/1.5S	535	42.4	1.87	4.35	-	226	319 +	0.71	270	0.84
BM1/2.0N	455	43.2	2.20	-	0.86	199	174 +	1.14	149	1.33
BM1/2.0S	455	43.2	2.20	-	-	177	174 +	1.02	149	1.19
BM2/2.0N	455	43.2	2.20	0.69	0.86	204	174 +	1.17	149	1.37
BM2/2.0S	455	43.2	2.20	0.69	-	185	174 +	1.06	149	1.24
Total							AVG	1.06	AVG	1.42
13							COV	0.13	COV	0.22

Table 6 Continued

Beam No.	d mm	f'_c MPa	a/d	$\rho_h f_{yh}$ MPa	$\rho_v f_{yv}$ MPa	$V_{bv,test}$ kN	Proposed method		ACI method	
							$V_{bv,calc}$ kN	$\frac{V_{bv,test}}{V_{bv,calc}}$	$V_{bv,calc}$ kN	$\frac{V_{bv,test}}{V_{bv,calc}}$
Foster and Gilbert (1998)										
B1.2-3	1124	80	0.76	1.71	3.95	1300	1120	1.16	1023	1.27
B2.0-1	624	83	1.32	2.18	3.95	795	632	1.26	551	1.44
B2.0-2	624	120	1.32	2.18	3.95	825	701	1.18	551	1.50
B2.0-3	624	78	1.32	2.18	3.95	700	621	1.13	551	1.27
B2.0B-5	624	89	1.32	-	-	585	562	1.04	551	1.06
B2.0C-6	624	93	1.32	-	5.90	730	662	1.10	551	1.33
B2.0D-7	624	104	1.32	-	3.95	720	658	1.09	387	1.31
B3.0-1	624	80	1.88	2.18	3.95	510	454 ⁺	1.12	387	1.32
B3.0-2	624	120	1.88	2.18	3.95	525	467 ⁺	1.12	387	1.36
B3.0-3	624	77	1.88	2.18	3.95	525	453 ⁺	1.16	387	1.36
B3.0B-4	624	89	1.88	-	-	435	422	1.03	387	1.12
Total							AVG	1.13	AVG	1.30
11							COV	0.06	COV	0.12
Lu <i>et al.</i> (2012)										
C1	900	34.6	0.83	-	-	1156	994	1.16	751	1.54
C2	900	34.6	0.83	2.92	2.64	1375	1235	1.11	883	1.56
C3	900	58.5	0.61	-	-	1542	1302	1.18	975	1.58
C4	900	58.5	0.61	1.48	-	1859	1418	1.31	975	1.91
C5	900	58.5	0.61	2.92	-	2018	1573	1.28	975	2.07
C6	900	67.8	0.83	-	-	1474	1347	1.09	1234	1.19
C7	900	67.8	0.83	2.92	-	1600	1627	0.98	1234	1.30
C8	900	67.8	0.83	-	2.64	1563	1402	1.11	1234	1.27
Total							AVG	1.15	AVG	1.55
8							COV	0.09	COV	0.20
Total							AVG	1.11		1.44
44							COV	0.09		0.18

⁺ Shear force according to the flexural strength [Eq. (13)]

model of the ACI Code (2011). The ratios of the measured shear strength to the calculated shear strength of the 44 deep beams are plotted with respect to the shear span-to-depth ratio (a/d) in Fig. 10. The proposed method consistently predicts the shear strength of deep beams with a/d

ratios between 0.56 and 2.20 (Fig. 10). More conservative but scattered predictions were obtained from the strut-and-tie model of the ACI Code (2011), as shown in Fig. 10.

The ratios of the measured shear strength to the calculated shear strength of 44 deep beams are plotted with respect to the compressive strength of concrete (f'_c) in Fig. 11. The proposed method consistently predicts the shear strength of deep beams with f'_c between 26.1 and 120 MPa (Fig. 11). More conservative but scattered predictions were obtained from the strut-and-tie model of the ACI Code (2011), as shown in Fig. 11.

The ratios of the measured shear strength to the calculated shear strength of 44 deep beams are plotted with respect to effective depth of deep beams in Fig. 12. The proposed method provided fairly uniform predictions of the shear strength of beams with effective depth ranging from 270 mm to 1124 mm (Fig. 12). More conservative but scattered predictions were obtained from the strut-and-tie model of the ACI Code (2011), as shown in Fig. 12. This is obvious, since the ACI Code method is used for design, while the proposed one has been built on the basis of the experimental results; hence it is more suitable to predict real behavior.

5. Conclusions

A total of 12 reinforced concrete deep beams were tested in this study. A method for determining the shear strengths of deep beams has been proposed. According to the test results in this study, the findings of previous tests, and the comparison of the predictions of the proposed method and the strut-and-tie model of the ACI Code (2011), the following conclusions can be drawn:

1. The shear strengths of deep beams increase with decreases in the shear span-to-depth ratios. The shear strengths can be effectively enhanced for deep beams reinforced with both horizontal and vertical stirrups.
2. The normalized shear strength is defined as the measured shear strength divided by the square root of the compressive strength of concrete and the shear area. The normalized shear strengths of deep beams decrease with increases in the shear span-to-depth ratios. The normalized shear strengths of deep beams did not increase proportionally with an increase in effective depth.
3. The proposed method can consistently predict the shear strength of deep beams with different shear span-to-depth ratios, compressive strengths of concrete and effective depth. More conservative but scattered predictions were obtained from the strut-and-tie model of the ACI Code.

Acknowledgements

This research study was partially sponsored by the National Science Council of the Republic of China under Project NSC 101-2221-E-163-005. The authors would like to express their gratitude for the support.

References

American Concrete Institute (2011), "Building code requirements for structural concrete (ACI 318-11) and

- Commentary (ACI 318R-11)", Farmington Hills, Mich.
- Kim, T.H., Cheon, J.H. and Shin, H.M. (2012), "Evaluation of behavior and strength of prestressed concrete deep beams using nonlinear analysis", *Comput. Concr.*, **9**(1), 63-79.
- Mihaylov, B.I., Bentz, E.C. and Collins, M.P. (2010), "Behavior of large deep beams subjected to monotonic and reversed cyclic shear", *ACI Struct. J.*, **107**(6), 726-734.
- Lu, W.Y., Hwang, S.J. and Lin, I.J. (2010), "Deflection prediction for reinforced concrete deep beams", *Comput. Concr.*, **7**(1), 1-16.
- Lu, W.Y., Lin, I.J. and Yu, H.W. (2012), "Shear strength of reinforced concrete deep beams", accepted by *ACI Struct. J.*.
- Russo, G., Venir, R., and Pauletta, M. (2005), "Reinforced concrete deep beams-shear strength model and design formula", *ACI Struct. J.*, **102**(3), 429-437.
- Tuchscherer, R., Birrcher, D., Huizinga, M. and Bayrak, O. (2010), "Confinement of deep beam nodal regions", *ACI Struct. J.*, **107**(6), 709-717.
- Tuchscherer, R., Birrcher, D., Huizinga, M. and Bayrak, O. (2010), "Distribution of stirrups across web of deep beams", *ACI Struct. J.*, **108**(1), 108-115.
- Yang, K.H. (2010), "Tests on light-weight concrete deep beams", *ACI Struct. J.*, **107**(6), 663-670.